Atmos. Chem. Phys. Discuss., 7, 9899–9924, 2007
www.atmos-chem-phys-discuss.net/7/9899/2007/

Atmospheric Chemistry and Physics Discussions

Nitrogen compounds and ozone in the stratosphere: comparison of MIPAS satellite data with the Chemistry Climate Model ECHAM5/MESSy1

C. Brühl[1], B. Steil[1], G. Stiller[2], B. Funke[3], and P. Jöckel[1]

[1]Max-Planck-Institute for Chemistry, Mainz, Germany
[2]Institute for Meteorology and Climate Research, Forschungszentrum Karlsruhe, Germany
[3]Instituto de Astrofísica de Andalucía, Granada, Spain

Received: 1 June 2007 – Accepted: 2 July 2007 – Published: 9 July 2007

Correspondence to: C. Brühl (chb@mpch-mainz.mpg.de)

Abstract

The chemistry climate model ECHAM5/MESSy1 (E5/M1) in a setup extending from the surface to 80 km with a vertical resolution of about 600 m near the tropopause with nudged tropospheric meteorology allows a direct comparison with satellite data of chemical species at the same time and location. Here we present results out of a transient 10 years simulation for the period of the Antarctic vortex split in September 2002, where data of MIPAS on the ENVISAT-satellite are available. For the first time this satellite instrument opens the opportunity, to evaluate all stratospheric nitrogen containing species simultaneously with a good global coverage, including the source gas N_2O which allows an estimate for NO_x-production in the stratosphere. We show correlations between simulated and observed species in the altitude region between 10 and 50 hpa for different latitude belts, together with the Probability Density Functions (PDFs) of model results and observations. This is supplemented by global charts on pressure levels showing the satellite data and the simulated data sampled at the same time and location. We demonstrate that the model in most cases captures the partitioning in the nitrogen family, the diurnal cycles and the spatial distribution within experimental uncertainty. There appears to be, however, a problem to reproduce the observed nighttime partitioning between N_2O_5 and NO_2 in the middle stratosphere.

1 Introduction

The nitrogen oxides are produced in the stratosphere by oxidation of the mostly biogenic source gas N_2O involving exited oxygen ($O(^1D)$. They provide the most important catalytic sink for ozone in the middle stratosphere and explain most of the seasonal cycle of total ozone in mid-latitudes (Brühl and Crutzen, 2000; Crutzen and Schmailzl, 1983). They are also responsible for the deactivation of chlorine from the CFCs in the lower stratosphere. In polar winter and spring the heterogeneous conversion of N_2O_5 and $ClONO_2$ inside the cold vortices to HNO_3 and subsequent denitrification by sed-

ACPD

7, 9899–9924, 2007

imentation of HNO_3 containing polar stratospheric cloud particles set the conditions for the ozone hole, the fast ozone destruction by halogens (Solomon, 1999). Here we present point-by-point comparisons between satellite data and a Chemistry Climate Model (CCM) simulation for all species of the NO_y-family simultaneously, including its source gas and dynamical tracer N_2O and ozone. Such a study might help to resolve problems present in many CCMs to correctly represent ozone in the lower and middle stratosphere compared to observations (Eyring et al., 2006).

2 MIPAS satellite data

MIPAS (Michelson Interferometer for Passive Atmospheric Sounding) is a Fourier transform spectrometer sounding the thermal emission of the earth's atmosphere between 685 and 2410 cm^{-1} (14.6–4.15 μm) in limb geometry (von Clarmann et al., 2003). It is operational on the ENVISAT since summer 2002. We use data from nominal observation mode (6–68 km). The field-of-view of the instrument at the tangent points is about 3 km in the vertical (up to 45 km) and 30 km in the horizontal (longitude). There are 14.3 orbits per day with measurements obtained about every 5° latitude at day and night at fixed local time (10 and 22 h) allowing for global coverage in one day. MIPAS was operational from July 2002 to March 2004 with full specification, in particular 0.035 cm^{-1} spectral resolution. MIPAS data used within this comparison are trace gas distributions retrieved with the IMK/IAA scientific processor based on re-processed Level-1b data (versions 4.61/62). Spectra containing cloud signal (mainly PSCs in this context) were identified using a method suggested by Spang et al. (2004) and have been excluded from further analysis. The general strategy and formalism of the retrieval is discussed in detail in von Clarmann et al. (2003). Data are available from July 2002 to March 2004 (however, not with complete coverage), except for NO, where only 3 consecutive days during the vortex split period in September 2002 and a few individual days in Winter 2003/2004 were processed up to now.

Typical error ranges in the lower stratosphere are: O_3 5% (Glatthor et al., 2006),

N_2O 7% (+7% high bias in tropics, Glatthor et al., 2005), HNO_3 10% (Wang et al., 2007; Mengistu Tsidu et al., 2005), NO_2 8% (night) – 18% (day) (Funke et al., 2005), NO 15% (day), N_2O_5 30% (Mengistu Tsidu et al., 2004), HO_2NO_2 19% (Stiller et al., 2007), $ClONO_2$ 7–13% (Höpfner et al., 2007). Improved non-LTE (local thermodynamic equilibrium) retrieval schemes (V8.0) for NO and NO_2 are used. These improvements include i) the use of log(VMR) instead of VMR (volume mixing ratio) in the retrieval vector, ii) revised non-LTE parameters for NO_2, and iii) joint-fitted VMR horizontal gradients at constant longitudes and latitudes. For NO retrievals, a revised set of spectral windows (micro-windows) is applied, which allows to measure NO down to altitudes of about 15 km.

3 The chemical circulation model ECHAM5/MESSy1

The atmospheric chemistry general circulation model ECHAM5/MESSy1 (E5/M1) is based on the 5th generation European Centre Hamburg GCM, a spectral general circulation model. The configuration applied for this study has a horizontal spectral resolution of T42 (or about 2.8° for the corresponding quadratic Gaussian grid) and 90 layers from the surface to about 80 km (1 Pa) (Giorgetta et al., 2006). The vertical resolution in the lower stratosphere is about 600 m. The model is able to calculate the Quasi-Biennial Oscillation internally. To allow for a direct and efficient comparison with observations of chemical species in the simulation used for the evaluation, tropospheric temperatures, vorticity and divergence and surface pressure are weakly nudged to ECMWF operational data (up to 200 hPa), see Jöckel et al. (2006). The results presented here are part of a transient simulation from 1996 to 2005. As main part of the Modular Earth Submodel System (MESSy, Jöckel et al., 2005), the model has fully interactive and flexible chemistry (Sander et al., 2005) with 104 species and about 250 homogeneous and heterogeneous reactions (+6 species and 40 reactions in cloud droplets), including interactive photolysis. The scheme covers the most important reactions and species from the troposphere to the mesosphere. The chemical

kinetics is mostly based on Sander et al. (2002). As in Stiller et al. (2007), infrared photolysis of HO_2NO_2 (short HNO_4) is included.

4 Point-by-point comparisons between model results and satellite data

For the comparison the model data points closest to the observations in space and time are selected. To avoid deviations due to the strong diurnal cycle of some nitrogen species the study is based on hourly output of the CCM for the selected period (instead of the 5 h setting in Jöckel et al., 2006).

4.1 Zonal averages

For the first time it is possible, to compare simulated global fields of N_2O and all major compounds of reactive nitrogen NO_y =HNO_3+NO+NO_2+2N_2O_5+HNO_4+$ClNO_3$ simultaneously with satellite data, using day and night data. First the zonal averages in the stratosphere, based on point-by-point comparisons, for the period from 23 to 25 September 2002 are shown in Fig. 1. Note that due to the peculiar dynamical situation of the split Antarctic vortex only the results north of about 50° S should be interpreted as typical. The upper panels in each group show the simulations, the lower panels the differences to the MIPAS data. Comparisons for other periods are in Jöckel et al. (2006).

From N_2O (upper left panels) it can be seen that the southern hemispheric subtropical barrier in the model appears to be shifted towards the equator and too strong causing too low N_2O in the subtropical and mid-latitude middle stratosphere. The transport barriers and their tightness or chemical distinctness have been analysed using the methods described in Sparling (2000). A shifted and too tight barrier is consistent with too high NO_y (lower right panels) in the southern subtropics, indicating processed air coming from above and separated from the tropics. Here the differences can reach 20%. The anti-correlation to N_2O in the middle stratosphere is also clearly visible in the

individual nitrogen compounds shown in the other panels of Fig. 1. The largest differences in N_2O and NO_y are in the lowermost stratosphere near the south-pole indicating a too weak downward motion in the model and maybe too much removal of HNO_3 by sedimentation of PSC particles. Since here the zonal average covers airmasses from inside and outside the vortices, including regions with strong horizontal gradients, differences can be also due to the different horizontal resolution of the observations and the model (see also next section). On the other hand the uncertainties of the satellite data are also largest there. In the northern hemispheric lower stratosphere the model agrees with the observations within their uncertainty range.

The data sets for day and night in the simulation and in the observations are consistent, as can be clearly seen from the fact that the spikes in NO, NO_2 and N_2O_5 (and weaker in HNO_4 and $ClNO_3$) appearing in a latitude belt around 8° N, where only daytime observations are available, vanish in total NO_y. The large differences in the partitioning between N_2O_5 and NO_x (=NO+NO_2) near the south-pole are mostly due to latitude mismatches between model data and observations which are critical at the terminator. The vertical difference patterns in ozone and HNO_4 are mostly related to the lower vertical resolution of the satellite data compared to the model. As shown in Jöckel et al. (2006) and Stiller et al. (2007) these differences would be reduced if the model data would be convolved with averaging kernels of the satellite data.

4.2 The southern vortex split, spatial distribution of nitrogen species

The lower stratospheric dynamics and the distribution of ozone is to a large extent controlled by planetary waves propagating from the troposphere. Nudging of the tropospheric meteorology enables the model to reproduce the major stratospheric warming and the remarkable split of the Antarctic vortex in September 2002. Here we focus on the altitude levels 50 hPa (interesting for polar heterogeneous chemistry) and 10 hPa (interesting for nitrogen summer chemistry and dynamics) and the same period as above.

The two remnants of the split vortex can be clearly seen in the observations and

simulations of HNO_3 and total reactive nitrogen NO_y at 50 hPa in Fig. 2. The features look rather similar except that in the observations the peaks of HNO_3 and NO_y near the edges of the vortices are more distinct than in the simulation.

Figure 3 shows the global view including also N_2O, O_3 and all the individual reactive nitrogen species, where the simultaneous observations are available for the first time. Here the upper panels of each group show the observations, the middle panels the model results and the lower panels the deviations. Since the footprints of the nighttime and daytime parts of the orbits (ascending and descending nodes) intersect on the maps, especially for NO and NO_2, the species with the largest diurnal variation, the maps appear noisy. For NO the zero values represent nighttime (second row, right panels); for NO_2 the higher values belong to the late evening measurements and data (second row, left panels), while the low values represent morning data and points inside the vortices.

The largest differences occur near the vortex edges due to resolution differences and slight offsets of the wave patterns. In general the model reproduces the observed distribution and partitioning of the nitrogen species, including the diurnal cycle and the denitrification in the vortices. The ozone depletion in the vortices by halogens is somewhat underestimated, mostly due to an underestimate of downward transport of chlorine into the lower stratosphere in Antarctic winter (Jöckel et al., 2006). The underestimate of downward transport is also indicated by too high N_2O inside the vortices (see also Fig. 1). On the other hand N_2O in southern mid-latitudes and between the vortex lobes is too low pointing to too much mixing at the vortex edge. For HNO_3, NO_2 and NO_y the eastern and western vortex lobes in the observations are more different concerning denitrification than in the model. HNO_4 is too high in southern mid-latitudes and between the vortices. NO, NO_2 and N_2O_5 show the largest differences near the south pole pointing to effects of the different horizontal resolution, or problems with the photolysis at large solar zenith angles. For chlorine nitrate the relatively large differences in the vortices are related to the coarser vertical resolution of the MIPAS data compared to the model and to the fact that the underestimated ozone depletion

favours the formation of chlorine nitrate instead of HCl when there are no more polar stratospheric clouds, i.e. in the chlorine deactivation phase. In both, observations and simulations there is still a $ClNO_3$-collar at the edges of the vortices (Höpfner et al., 2004).

In the results for 10 hPa shown in Fig. 4 the differences are largest near the southern subtropical barrier which appears to be shifted towards the equator in the model in this altitude region as can be seen from too low N_2O and too high NO_y (including HNO_3) at about 15° S (compare Fig. 1). In the model N_2O in the southern mid-latitudes is low biased because of a too tight subtropical barrier. In mid-latitudes the partitioning of NO_y is well represented in the simulation. The diurnal cycle for NO, NO_2 and N_2O_5 can be clearly seen from the strongly varying colours along latitude circles due to the intersecting daytime (descending) and nighttime (ascending) nodes of the orbit. Here the larger values belong to daytime for NO and nighttime for NO_2 and N_2O_5, with a larger amplitude than for 50hPa shown in Fig. 3. At the south-pole the partitioning between N_2O_5 and $NO+NO_2$ is shifted towards $NO+NO_2$ in the model because of permanent N_2O_5 photolysis while the observations are mostly taken around 86° S where a day night cycle is present (the different horizontal resolution can cause a mismatch of more than 2° latitude). There are also large differences near the western vortex lobe near the south pole in NO_y probably due to differences in the wave patterns. The simulated reservoir species $ClONO_2$ is high in the Arctic, while HNO_3 is low there as already seen in Fig. 1. In the Antarctic the observed split vortex is well represented in the simulations, except for a maybe slightly overestimated denitrification from overestimated PSCs there (see NO_y , HNO_3, NO_2 and $ClNO_3$ in Fig. 4). The reason for the low model HNO_3 in the vortices can also be the neglect of a new reaction leading from NO_x to HNO_3: $NO+HO_2 \rightarrow HNO_3$ (Butkovskaya et al., 2005). Inclusion of this reaction in a sensitivity simulation leads to better agreement for HNO_3 and N_2O_5 in Fig. 4 because this provides a significant source for HNO_3 (and a sink for NO_x) in the middle and upper stratosphere where the vortex air originates from. HNO_3 at the vortices increases with the additional reaction pathway by about 0.5 ppbv.

4.3 Comparison based on correlations and probability density functions

Instead of comparing patterns as in the previous section, here we analyse point-by-point correlations and probability density functions (PDFs) for mixing ratios in latitude bins. As examples we show in Fig. 5 the lower stratosphere at high southern latitudes and in Fig. 6 the middle stratosphere in northern mid-latitudes, corresponding to Figs. 3 and 4. The first example is selected to look for the effects of dynamics and heterogeneous chemistry, the second for typical late summer gas-phase chemistry.

In high southern latitudes at 50 hPa (Fig. 5) the PDFs for observations and simulation are rather similar, except for the low bias of N_2O outside the vortices in the model (as discussed before) and more high HNO_3 and NO_y values in the observations. The vortex peaks in the PDFs for N_2O and NO_y in the model data and the observations are close together while the peaks for non-vortex air (high values) are different. For NO the zero nighttime values have a probability of about 50% in the model data and the observations which is consistent with equinox conditions. For NO_2, N_2O_5 and HNO_4 zero values are more likely in the model than in the observations. Comparison with Fig. 3 reveals that these low values occur in vortex air pointing to slight differences in heterogeneous chemistry.

In the middle stratosphere of the northern mid-latitudes (10 hPa, Fig. 6) the variability of HNO_3, NO and NO_y is larger in the observations than in the simulation. As a consequence, for NO_y the width of the PDF of the observations is much larger than the one for the model, however, the PDFs in model and observations peak around the same value of about 16 ppbv. This behaviour implies relatively low correlations. In NO_2 and NO in observations and simulations the clusters related to the diurnal cycle are visible, however the nighttime peak for NO_2 in the model is low biased. For N_2O_5 the model tends to overestimate the diurnal cycle in the middle stratosphere which was already indicated at 50 hPa. The high bias at nighttime (22 h local time) is consistent with the diurnal behaviour of NO_2. It can neither be explained by more NO_3 formation due to about 3% too high ozone in this region (Fig. 1), nor by a temperature

bias. The diurnal sampling of the simulation data should give only a small contribution to the differences, since for the selected equinox conditions the observations are about 4 h apart from sunset or sunrise (except for the poles). Inclusion of NO+ $HO_2 \rightarrow HNO_3$ and the channel to NO_3+NO+O in N_2O_5 photolysis (which was neglected in the setup described in Jöckel et al., 2006) reduces the discrepancies for the morning data. It is still unresolved, however, if the representation of the chemistry in the model is incomplete, or a problem with absorption cross sections or quantum yields of N_2O_5 photolysis is the reason, or a problem with the satellite observations (MIPAS might be high against ACE, Höpfner, personal communication) causes the discrepancies. We have performed several sensitivity studies using additional pathways in the photolysis calculations or changes in reaction coefficients given in the most recent recommendation (Sander et al., 2006), without achieving a significantly better agreement with the observations for the late evening values of NO_2 and N_2O_5.

5 Production of reactive nitrogen from N_2O

MIPAS N_2O, O_3 and temperature together with the $O(^1D)/O_3$ ratio from E5/M1 are used to derive the chemical production of NO_y. Fig. 7 shows the production at 10 h local time at the satellite points at 2 altitudes. The values are about 3 times the diurnal average which is consistent with the diurnal cycle of $O(^1D)$. The individual data-points show a variability due to dynamics in N_2O and due to cloud effects on the photolysis of O_3 leading to $O(^1D)$. The patterns are similar to the average production calculated purely from the model in the lower panels, supporting the consistency between N_2O and NO_y already seen from the previous figures. Clearly visible are again the two lobes of the Antarctic vortex where NO_y-production is low due to low N_2O. The NO_y-production integrated over the stratosphere (100 to 1 hPa) based on model simulations is shown in Fig. 8. Its spatial patterns are dominated by the region between about 10 and 20 hPa.

6 Conclusions

ECHAM5/MESSy1 with nudged tropospheric meteorology captures most of the features of nitrogen species observed by MIPAS on ENVISAT in the lower stratosphere, including the 2002 Antarctic vortex split and the diurnal variation of NO and NO_2. MIPAS allows a complete evaluation of the NO_y-family and the nitrogen budget, the partitioning of nitrogen species in the model especially in mid-latitudes and tropics agrees well with observations (if NIR-photolysis of HO_2NO_2 is included). The differences in the diurnal behaviour of N_2O_5 and NO_2 in the middle stratosphere, however, cannot be explained by model dynamics, resolution differences or given uncertainties in the chemistry used in the calculations. There might be the need for more laboratory work.

The model underestimates the downward transport in the lowermost parts of the vortices with the consequence of underestimated ozone depletion by reactive halogens, and a shift to chlorine-nitrate in the chlorine partitioning. Another model feature is the too tight southern subtropical barrier causing too low N_2O and too high NO_y in the middle stratosphere of southern mid-latitudes. Here appears to be a need to improve the model dynamics, particularly the forcing by gravity waves.

Acknowledgements. Parts of this study were supported by the European Union Integrated Project SCOUT-O3.

References

Brühl, C. and Crutzen, P. J.: NO_x-catalyzed ozone destruction and NO_x activation at midlatitudes to high latitudes as a main cause of the spring to fall ozone decline in the Northern Hemisphere, J. Geophys. Res., 105, 12 163–12 168, 2000. 9900

Butkovskaya, N. I., Kukui, A., Pouvesle, N., and Le Bras, G.: Formation of nitric acid in the gas-phase HO_2+NO reaction: Effects of temperature and water vapor, J. Phys. Chem. A, 109, 6509–6520, 2005. 9906

Crutzen, P. J. and Schmailzl, U.: Chemical budgets of the stratosphere, Planet. Space Sci., 31, 1009–1032, 1983. 9900

Eyring, V., Butchart, N., Waugh, D. W., Akiyoshi, H., Austin, J., Bekki, S., Bodeker, G. E., Boville, B. A., Brühl, C., Dameris, M., Deushi, M., Fioletov, V. E., Frith, S. M., Garcia, R. R., Gettelman, A., Giorgetta, M. A., Grewe, V., Jourdain, L., Kinnison, D. E., Mancini, E., Manzini, E., Marchand, M., Marsh, D. R., Nagashima, T., Newman, P. A., Nielsen, J. E., Pawson, S., Pitari, G., Plummer, D. A., Rozanov, E., Schraner, M., Shepherd, T. G., Shibata, K., Stolarski, R. S., Struthers, H., Tian, W., and Yoshiki, M.: Assessment of temperature, trace species, and ozone in chemistry-climate model simulations of the recent past, J. Geophys. Res., 111, D22308, doi:10.1029/2006JD007327, 2006. 9901

Funke, B., López-Puertas, M., von Clarmann, T., Stiller, G. P., Fischer, H., Glatthor, N., Grabowski, U., Höpfner, M., Kellmann, S., Kiefer, M., Linden, A., Mengistu Tsidu, G., Milz, M., Steck, T., and Wang, D. Y.: Retrieval of stratospheric NO_x from 5.3 and 6.2 μm nonlocal thermodynamic equilibrium emissions measured by Michelson Interferometer for Passive Atmospheric Sounding (MIPAS) on Envisat, J. Geophys. Res., 110, D09302, doi:10.1029/2004JD005225, 2005. 9902

Giorgetta, M. A., Manzini, E., Roeckner, E., Esch, M., and Bengtsson, L.: Climatology and forcing of the quasi-biennial oscillation in the MAECHAM5 model, J. Climate, 19, 3882–3901, 2006. 9902

Glatthor, N., von Clarmann, T., Fischer, H., Funke, B., Grabowski, U., Höpfner, M., Kellmann, S., Kiefer, M., Linden, A., Milz, M., Steck, T., Stiller, G. P., Mengistu Tsidu, G., and Wang, D. Y.: Mixing processes during the Antarctic vortex split in September/ October 2002 as inferred from source gas and ozone distributions from ENVISAT-MIPAS, J. Atmos. Sci., 62, 787–800, 2005. 9902

Glatthor, N., von Clarmann, T., Fischer, H., Funke, B., Gil-López, S., Grabowski, U., Höpfner, M., Kellmann, S., Linden, A., López-Puertas, M., Mengistu Tsidu, G., Milz, M., Steck, T., Stiller, G. P., and Wang, D. Y.: Retrieval of stratospheric ozone profiles from MIPAS/ENVISAT limb emission spectra: a sensitivity study, Atmos. Chem. Phys., 6, 2767–2781, 2006, http://www.atmos-chem-phys.net/6/2767/2006/. 9901

Höpfner, M., von Clarmann, T., Fischer, H., Glatthor, N., Grabowski, U., Kellmann, S., Kiefer, M., Linden, A., Mengistu Tsidu, G., Milz, M., Steck, T., Stiller, G. P., Wang, D.-Y., and Funke, B.: First spaceborne observations of Antarctic stratospheric $ClONO_2$ recovery: Austral spring 2002, J. Geophys. Res., 109, D11308, doi:10.1029/2004JD004609, 2004. 9906

Höpfner M., von Clarmann, T., Fischer, H., Funke, B., Glatthor, N., Grabowski, U., Kellmann, S., Kiefer, M., Linden, A., Milz, M., Steck, T., Stiller, G. P., Bernath, P., Blom, C. E., Blumenstock,

T., Boone, C., Chance, K., Coffey, M. T., Friedl-Vallon, F., Griffith, D., Hannigan, J. W., Hase, F., Jones, N., Jucks, K. W., Keim, C., Kleinert, A., Kouker, W., Liu, G. Y., Mahieu, E., Mellqvist, J., Mikuteit, S., Notholt, J., Oelhaf, H., Piesch, C., Reddmann, T., Ruhnke, R., Schneider, M., Strandberg, A., Toon, G., Walker, K. A., Warneke, T., Wetzel, G., Wood, S., and Zander, R.: Validation of MIPAS $ClONO_2$ measurements, Atmos. Chem. Phys. 7, 257–281, 2007. 9902

Jöckel, P., Sander, R., Kerkweg, A., Tost, H., and Lelieveld, J.: Technical Note: The Modular Earth Submodel System (MESSy) – a new approach towards Earth System Modeling, Atmos. Chem. Phys., 5, 433–444, 2005, http://www.atmos-chem-phys.net/5/433/2005/. 9902

Jöckel, P., Tost, H., Pozzer, A., Brühl, C., Buchholz, J., Ganzeveld, L., Hoor, P., Kerkweg, A., Lawrence, M. G., Sander, R., Steil, B., Stiller, G. , Tanarhte, M., Taraborrelli, D., van Aardenne, J., and Lelieveld, J.: The atmospheric chemistry general circulation model ECHAM5/MESSy1: consistent simulation of ozone from the surface to the mesosphere. Atmos. Chem. Phys., 6, 5067–5104, 2006, http://www.atmos-chem-phys.net/6/5067/2006/. 9902, 9903, 9904, 9905, 9908

Mengistu Tsidu, G., Stiller, G. P., von Clarmann, T., Funke, B., Höpfner, M., Fischer, H., Glatthor, N., Grabowski, U., Kellmann, S., Kiefer, M., Linden, A., López-Puertas, M., Milz, M., Steck, T., and Wang, D. Y.: NO_y from Michelson Interferometer for Passive Atmospheric Sounding on Environmental Satellite during the Southern Hemisphere polar vortex split in September/October 2002, J. Geophys. Res., 110, D11301, doi:10.1029/2004JD005322, 2005. 9902

Mengistu Tsidu, G., von Clarmann, T., Stiller, G. P., Höpfner, M., Fischer, H., Glatthor, N., Grabowski, U., Kellmann, S., Kiefer, M., Linden, A., Milz, M., Steck, T., Wang, D.-Y., and Funke, B.: Stratospheric N_2O_5 in the austral spring 2002 as retrieved from limb emission spectra recorded by the Michelson Interferometer for Passive Atmospheric Sounding (MIPAS), J. Geophys. Res., 109, D18301, doi:10.1029/2004JD004856, 2004. 9902

Sander, R., Kerkweg, A., Jöckel, P., and Lelieveld, J.: Technical Note: The new comprehensive atmospheric chemistry module MECCA, Atmos. Chem. Phys., 5, 445–450, 2005, http://www.atmos-chem-phys.net/5/445/2005/. 9902

Sander, S. P., Finlayson-Pitts, B. J., Friedl, R. R., Golden, D. M., Huie, R. E., Kolb, C. E., Kurylo, M. J., Molina, M. J., Moortgat, G. K., Orkin, V. L., and Ravishankara, A. R.: Chemical Kinetics and Photochemical Data for Use in Atmospheric Studies, Evaluation Number 14, JPL Publication 02-25, Jet Propulsion Laboratory, Pasadena, 2002. 9903

Sander, S. P., Friedl, R. R., Golden, D. M., Kurylo, M. J., Moortgat, G. K., Keller-Rudek, H.,

Wine, P. H., Ravishankara, A. R., Kolb, C. E., Molina, M. J., Finlayson-Pitts, B. J., Huie, R. E., and Orkin, V. L.: Chemical kinetics and photochemical data for use in atmospheric studies, Evaluation Number 15, JPL Publication 06-2, Jet Propulsion Laboratory, Pasadena, 2006. 9908

Solomon, S.: Stratospheric ozone depletion: A review of concepts and history, Rev. Geophys., 37(3), 275–316, 1999. 9901

Spang, R., Remedios, J. J., and Barkley, M. P.: Colour indices for the detection and differentiation of cloud types in infra-red limb emission spectra, Adv. Space Res., 33, 1041–1047, 2004. 9901

Sparling, L. C.: Statistical perspectives on stratospheric transport, Rev. Geophys., 38, 417–436, 2000. 9903

Stiller, G. P., von Clarmann, T., Brühl, C., Fischer, H., Funke, B., Glatthor, N., Grabowski, U., Höpfner, M., Jöckel, P., Kellmann, S., Kiefer, M., Linden, A., López-Puertas, M., Mengistu Tsidu, G., Milz, M., Steck, T., and Steil, B.: Global distributions of HO_2NO_2 as retrieved from observations of the Michelson Interferometer for Passive Atmospheric Sounding (MIPAS), J. Geophys. Res., 112, D09314, doi:10.1029/2006JD007212, 2007. 9902, 9903, 9904

von Clarmann, T., Glatthor, N., Grabowski, U., Höpfner, M., Kellmann, S., Kiefer, M., Linden, A., Mengistu Tsidu, G., Milz, M., Steck, T., Stiller, G. P., Wang, D. Y., Fischer, H., Funke, B., Gil-López, S., and López-Puertas, M.: Retrieval of temperature and tangent altitude pointing from limb emission spectra recorded from space by the Michelson Interferometer for Passive Atmospheric Sounding (MIPAS), J. Geophys. Res., 108(D23), 4736, doi:10.1029/2003JD003602, 2003. 9901

Wang, D. Y., Höpfner, M., Mengistu Tsidu, G., Stiller, G. P., von Clarmann, T., Fischer, H., Blumenstock, T., Glatthor, N., Grabowski, U., Hase, F., Kellmann, S., Linden, A., Milz, M., Oelhaf, H., Schneider, M., Steck, T., Wetzel, G., López-Puertas, M., Funke, B., Koukouli, M. E., Nakajima, H., Sugita, T., Irie, H., Urban, J., Murtagh, D., Santee, M. L., Toon, G., Gunson, M. R., Irion, F. W., Boone, C. D., Walker, K., and Bernath, P. F.: Validation of nitric acid retrieved by the IMK-IAA processor from MIPAS/ENVISAT measurements. Atmos. Chem. Phys., 7, 721–738, 2007, http://www.atmos-chem-phys.net/7/721/2007/. 9902

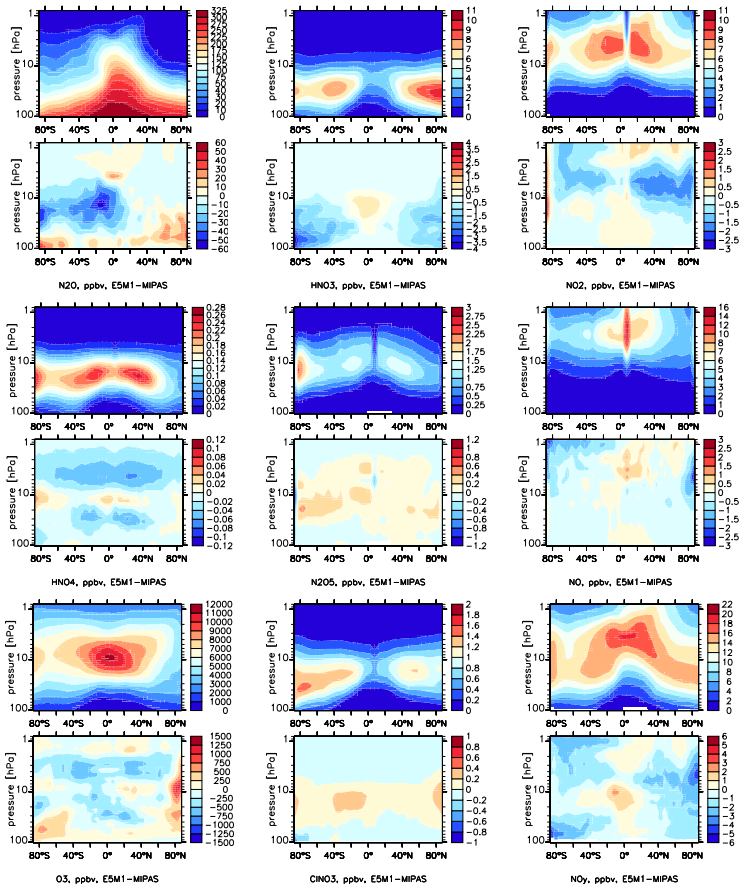

Fig. 1. Simulated zonal averages at MIPAS datapoints (upper panel) and differences to MIPAS (lower panel) for 23–25 Sept. 2002: upper two rows N_2O, HNO_3, NO_2, middle two rows HNO_4, N_2O_5, NO, lower two rows O_3, $ClNO_3$ and NO_y. Note that at 8° N MIPAS has only daytime data.

ACPD
7, 9899–9924, 2007

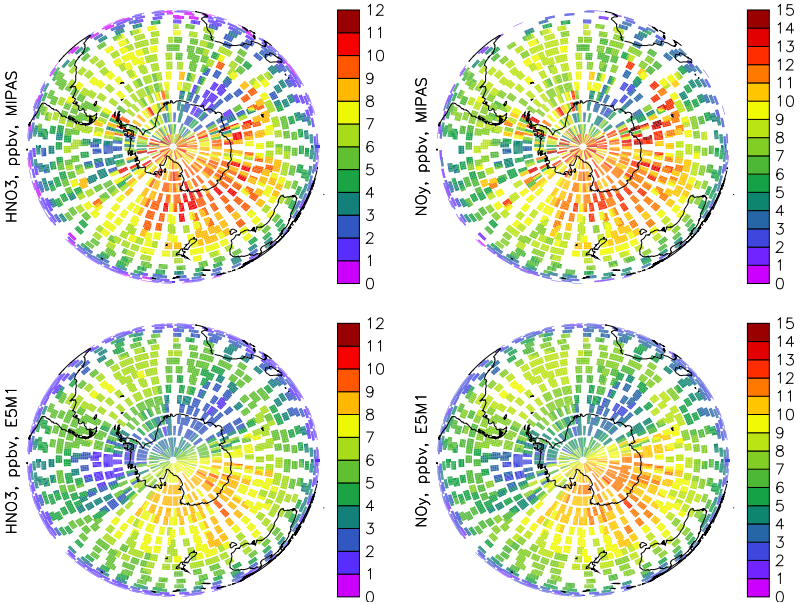

Fig. 2. HNO_3 and NO_y at 50 hPa, showing the split vortex over Antarctica. Upper panels MIPAS observations, lower panels simulations with E5/M1 for 23–25 September 2002.

ACPD
7, 9899–9924, 2007

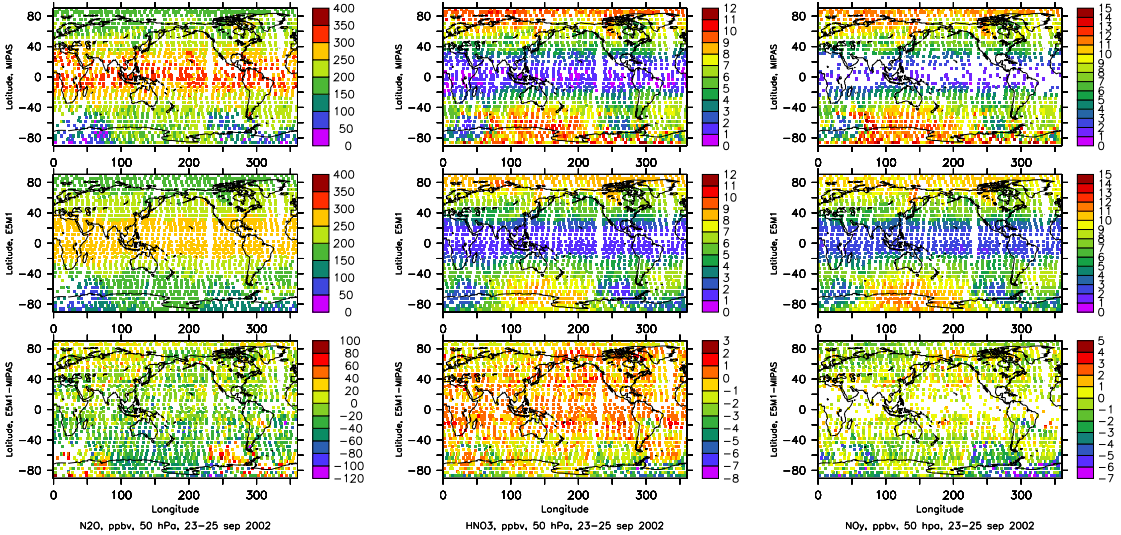

Fig. 3. N_2O, HNO_3, NO_y (first 3 rows), NO_2, N_2O_5, NO (second 3 rows), O_3, $ClONO_2$ ($ClNO_3$) and HNO_4 (third 3 rows) at 50hPa for 23–25 September 2002 as observed by MIPAS (upper panels of each group), simulated by ECHAM5/MESSy1 (middle panels) and deviations of the model to MIPAS (point-by-point in space and time, lower panels of each group).

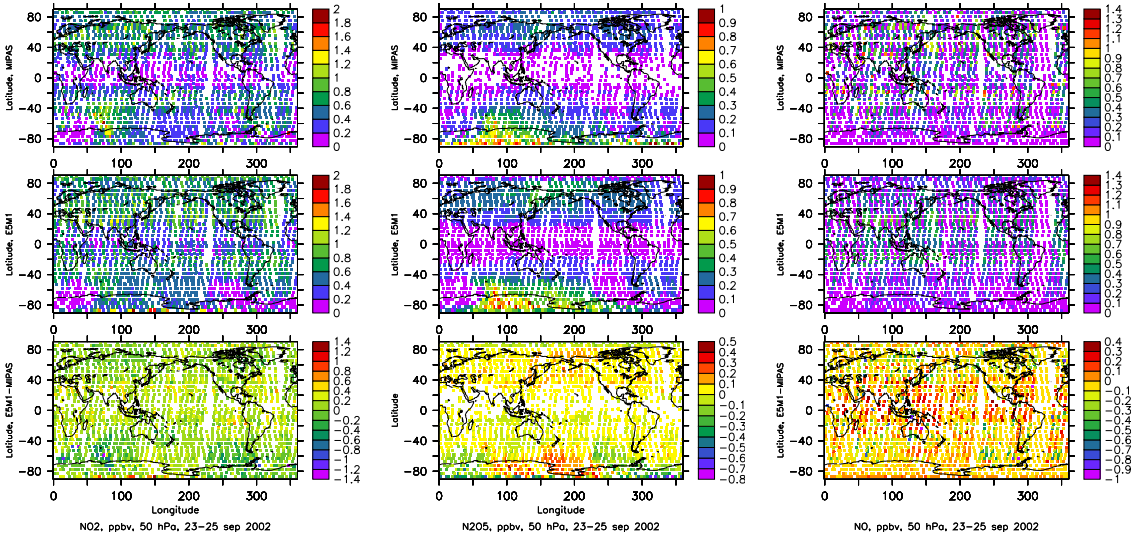

Fig. 3. Continued.

ACPD
7, 9899–9924, 2007

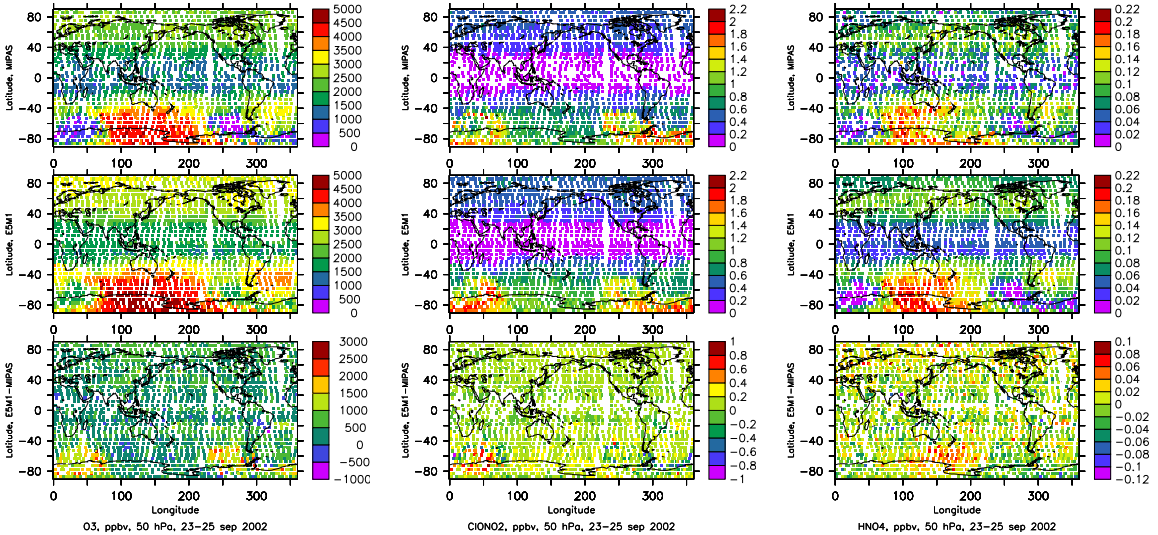

Fig. 3. Continued.

ACPD
7, 9899–9924, 2007

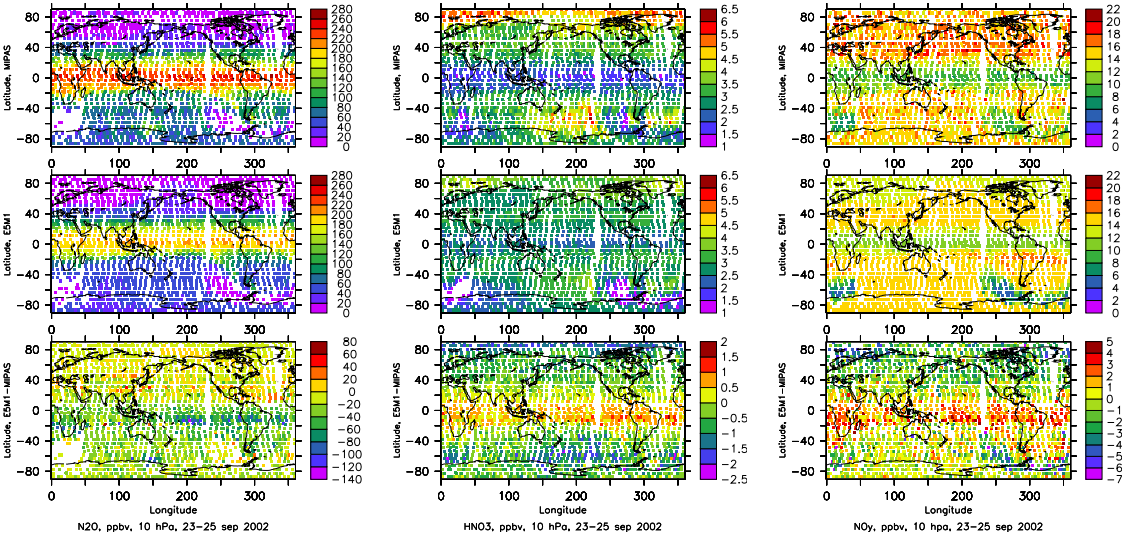

Fig. 4. As Fig. 3 but for 10 hPa.

ACPD
7, 9899–9924, 2007

EGU

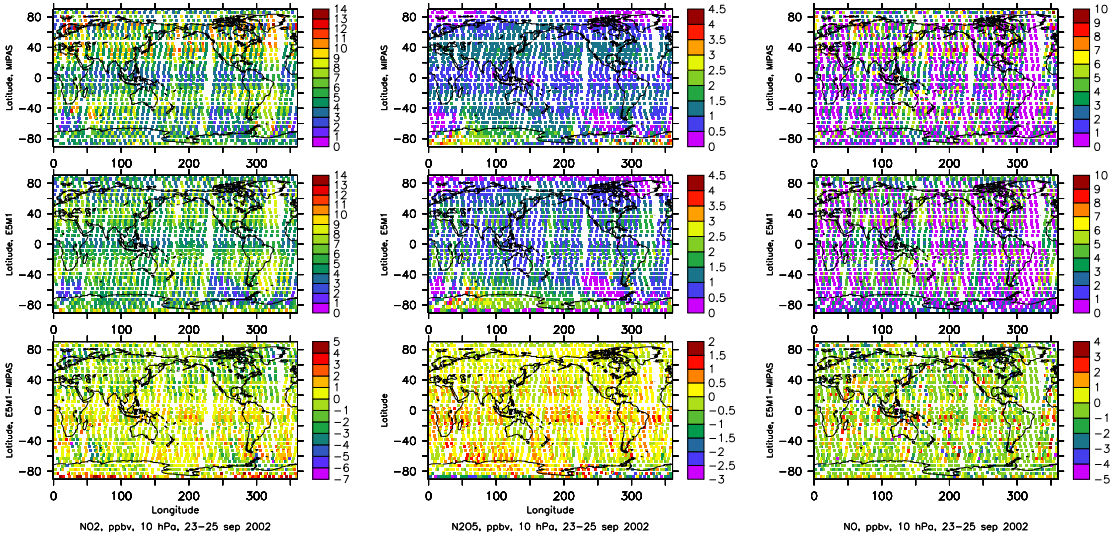

Fig. 4. Continued.

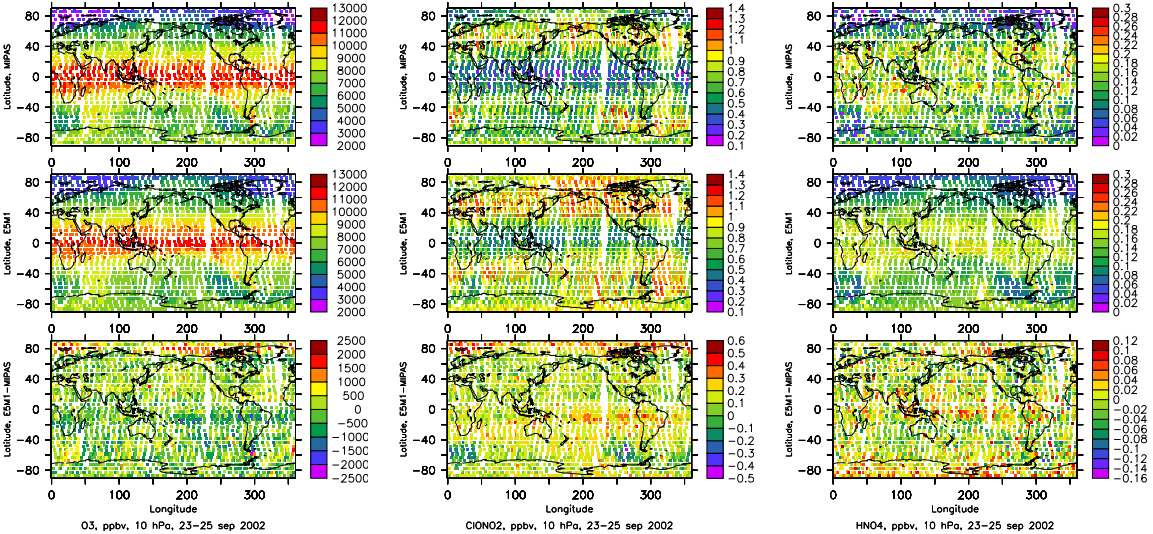

Fig. 4. Continued.

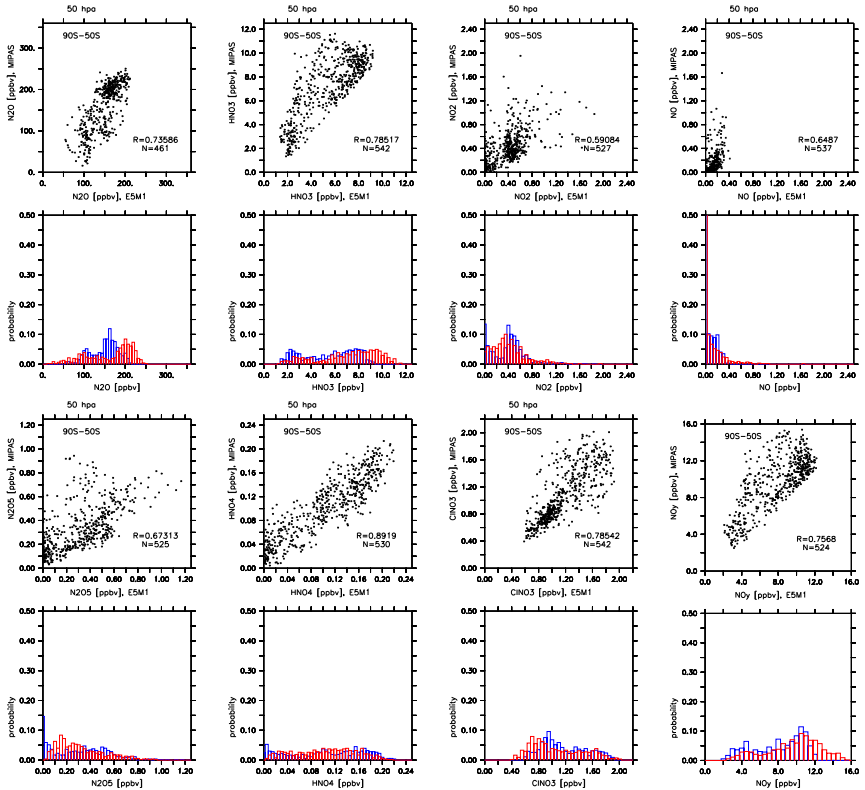

Fig. 5. Point-by-point correlations of MIPAS data to ECHAM5/MESSy results and probability density functions (PDF) for 50 to 90° S at 50 hPa, 23–25 September 2002. MIPAS red, model blue. Upper rows: N_2O, HNO_3, NO_2, NO; lower rows: N_2O_5, HNO_4, $ClONO_2$ and total nitrogen NO_y. R is the correlation coefficient, N the number of data points in the latitude bin. For the PDFs the bins for the observations are shifted by 10% of the binsize for better visibility.

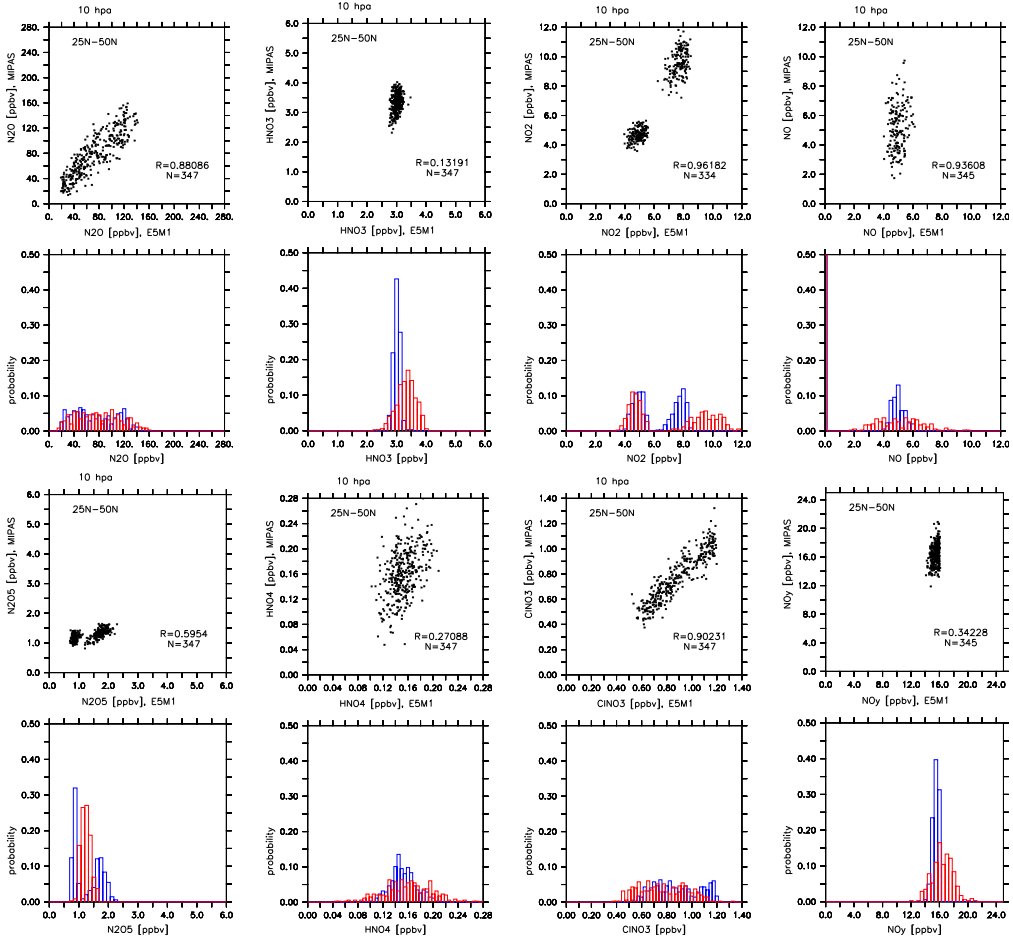

Fig. 6. As Fig. 5 but for 25 to 50° N at 10 hPa, 23–25 September 2002. Note the zero values for nighttime NO. MIPAS red, model blue.

ACPD
7, 9899–9924, 2007

EGU

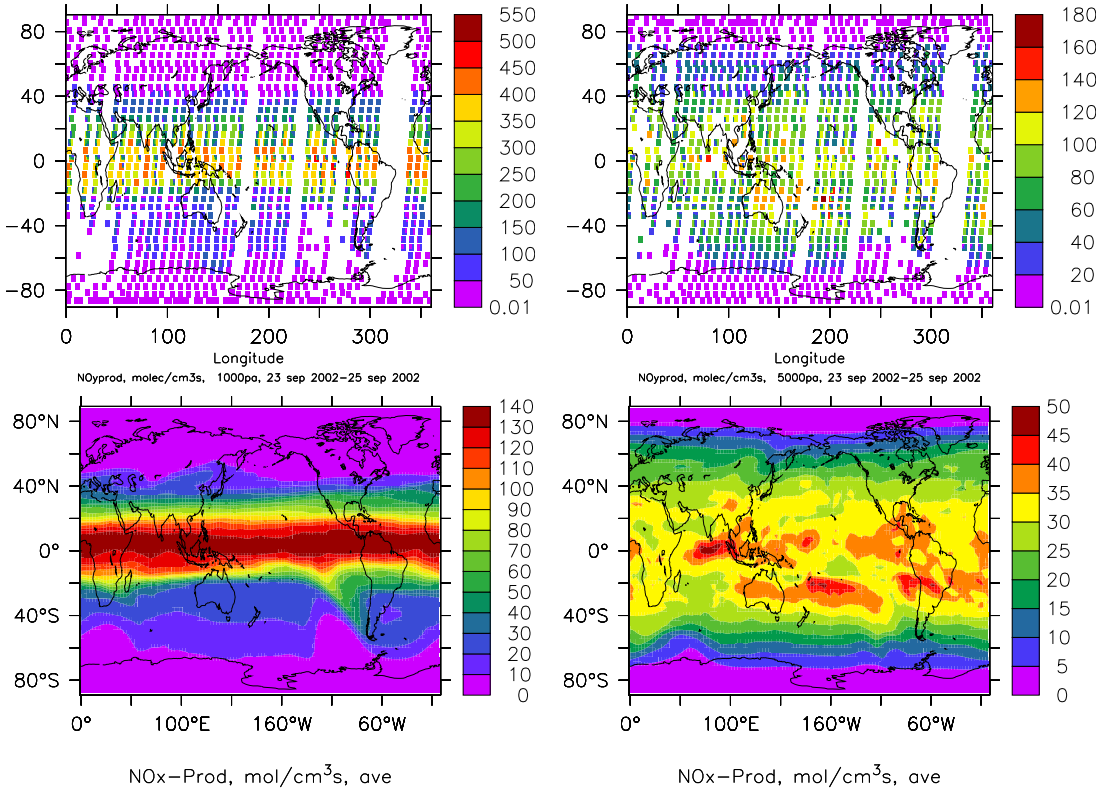

Fig. 7. Upper panels: NO_y-production at 10:00 h local time (about 3 times the diurnal average) and 22:00 h local time (only polar day near south-pole) based on MIPAS N_2O, O_3, T and the $O(^1D)/O_3$ ratio from the model at the data points. 10 hPa left, 50 hPa right. Lower panels: Diurnal average from the simulation only for same period (23–25 September 2002).

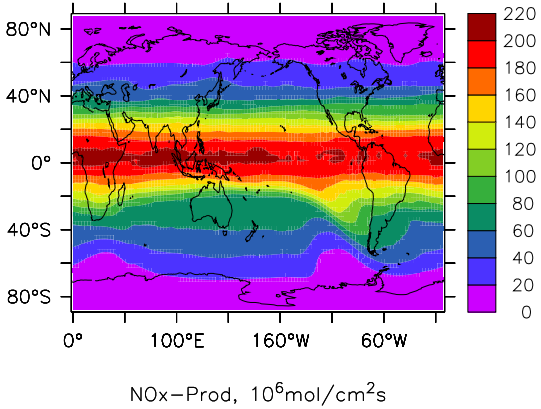

Fig. 8. NO_y-production integrated over the stratosphere (1–100 hPa, 23–25 September 2002), based on E5/M1 simulations.